Characterization of MU-MIMO Channels
Using the Spectral Divergence Measure

Florian Kaltenberger
Eurecom
2229, Route des Cretes - B.P. 193
06904 Sophia Antipolis, France

Laura Bernadó, Thomas Zemen
ftw. Forschungszentrum Telekommunikation Wien
Donau-City-Strasse 1
1220 Wien, Austria

Phone: +33 4 93 00 81 86
Fax: +33 4 93 00 82 00
Email: florian.kaltenberger@eurecom.fr

Abstract

In this work we apply the spectral divergence to characterize the (dis-)similarity of different links in wide-band multi-user multiple-input multiple-output (MU-MIMO) channels. The spectral divergence measures the distance between strictly positive, non-normalized spectral densities, such as the power delay profile. The measurement data has been acquired using Eurecom's MIMO Openair Sounder (EMOS). The EMOS can perform real-time MIMO channel measurements synchronously over multiple users. For this work we have used a line-of-sight measurement with two transmit antennas and two users with two antennas each. We compare the spectral divergence of different links with respect to the distance of the users. We find that the spectral divergence can be quite low when the users are close together. These findings are important for MU-MIMO precoding and scheduling algorithms. [1]

I. INTRODUCTION

In a cellular network, cooperation between users can be used to greatly increase power efficiency, reliability and throughput. Cooperation can be achieved by using the antennas of multiple users to form a virtual antenna array and by using MIMO transmission/reception techniques. The development and realistic performance assessment of such distributed MIMO systems requires measurement and characterization of the different channel links in these systems. To this end, only a limited amount of channel measurements and analysis of such distributed MIMO systems are available.

In [1], [2], [3] realistic MU-MIMO channel measurements have been obtained using Eurecom's MIMO Openair Sounder (EMOS) [4]. The EMOS can perform real-time channel measurements synchronously over multiple users moving at vehicular speed. The measured channels are used to calculate the capacity of the MU-MIMO broadcast channel. One of the findings of [2] was that the performance of MU-MIMO precoding drops drastically when the users are close together in an outdoor scenario. It was further noted that this decline in performance is due to the strong correlation at the transmitter.

The correlation measures the co-linearity between quantities. In the case of [2] these were frequency responses of the links in a MU-MIMO channel. An alternative correlation measure is the spectral divergence (SD) [5]. It measures the distance between strictly positive, non-normalized spectral densities. In this work it is applied to the power delay profiles of the different links in a MU-MIMO channel. Thus we are able to better characterize the correlation in wideband channels.

The SD was used in [6] to characterize the similarity between scattering functions of different links in a MIMO channel and in [7] to characterize the similarity between local scattering functions of a time- and frequency-selective vehicular channel.

Related channel measurements have been described in [8]. The measurements were conducted using a MEDAV-LUND channel sounder with its corresponding receiver as well as the receiver of an Elektrobit channel sounder. The two receivers are perfectly synchronized. The authors present capacity with interference results, based on the dynamic multilink measurements, as well as path-loss and delay spreads for the measured scenarios.

This paper is organized as follows. In Section II, the EMOS measurement platform is described in some detail. In Section III we describe the post processing steps and parameter extraction.

(a) CBMIMO1 Card   (b) Panorama Antennas   (c) Powerwave Antenna
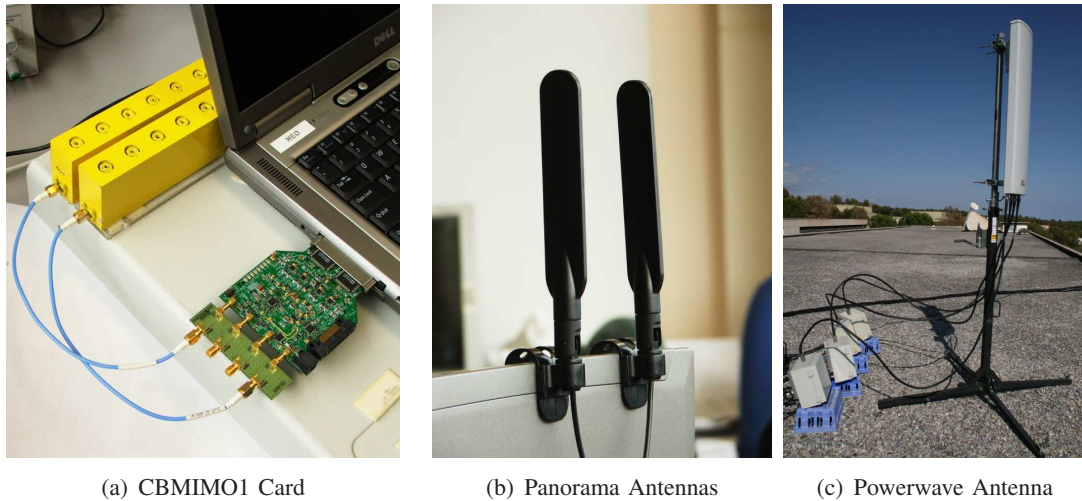
Fig. 1.   EMOS base-station and user equipment.

In Section IV we describe the measurements and their results. Finally conclusions are drawn in Section V.

II. DESCRIPTION OF THE MEASUREMENT PLATFORM AND SYSTEM MODEL

A. Hardware

The Eurecom MIMO Openair Sounder (EMOS) is based on the OpenAirInterface hardware/ software development platform at Eurecom[2]. The platform consists of a BS and one or more UEs. The BS as well as the UEs consist of a laptop computer with Eurecom's dual-RF CardBus/PCMCIA card called CBMIMO1 (see Fig. 1(a)). The RF section of the CBMIMO1 cards is time-division duplex and operates at 1.900-1.920 GHz with 5 MHz channels. EURECOM has a frequency allocation for experimentation around its premises in Sophia-Antipolis.

At the BS the CBMIMO1 card is connected to power amplifiers which are further connected to a Powerwave 3G broadband antenna (part no. 7760.00). The antenna is composed of four elements which are arranged in two cross-polarized pairs (see Fig. 1(c)). However, at the moment only two out of those four elements are used (see Section IV for details). At the UE, two clip-on 3G Panorama Antennas (part no. TCLIP-DE3G, see Fig. 1(b)) are directly connected to the antennas (with an optional filter to reduce adjacent band interference).

The platform is designed for a full software-radio implementation, in the sense that all protocol layers run on the host PCs under the control of a Linux real time operation system.

B. Sounding Signal

The EMOS is using an OFDM modulated sounding sequence. The most important parameters are given in Table I. The hardware at the transmitter automatically adds a cyclic suffix to each OFDM symbol. Thus, one OFDM symbol consists of $N_d + N_c$ samples and is 41,7 μs long.

One transmit frame consists of 64 OFDM symbols and contains a synchronization symbol (SCH), a broadcast data channel (BCH) comprising 7 OFDM symbols, a guard interval, and 48 pilot symbols used for channel estimation (see Fig. 2). The total length of a frame is 2.667ms,

---

[2]http://www.openairinterface.org

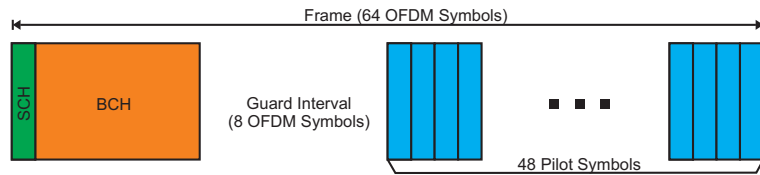| Parameter	Value	Description
f_c	1917.6 MHz	Center Frequency
f_s	7.68 MHz	Sampling Rate
N_s	64	Number of OFDM Symbols per TTI
N_d	256	Number of OFDM Carriers
N_c	64	Number of Prefix Samples
N_z	96	Number of Zero Carriers
$N_u = N_d - N_z$	160	Number of Usefull Carriers
$B = \frac{N_u}{N_d} f_s$	4.8 MHz	Usefull Bandwidth

TABLE I
OFDM PARAMETERS.

Fig. 2. Frame structure of the OFDM Sounding Sequence.

which results in a snapshot rate of 375 Hz and thus a max. resolvable Doppler of 187.5 Hz ($\approx$ 105 km/h). The pilot symbols are taken from a pseudo-random QPSK sequence defined in the frequency domain. The subcarriers of the pilot symbols are multiplexed over the four transmit antennas to ensure orthogonality in the spatial domain. The BCH contains the frame number of the transmitted frame that is used for synchronization among the UEs. The BCH uses QPSK modulation and a rate 1/2 convolutional code and includes a cyclic redundancy check (CRC).

C. Synchronization

Transmitter and receiver must be synchronized in order to conduct usefull measurements. Synchronization is taking place at three different levels, which are described below.

1) Initial Synchronization: Initial synchronization is performed using a sliding window correlator on the SCH symbol in the frequency domain. After detection of the SCH, the BCH is decoded. Synchronization is declared only if the BCH can be detected successfully (CRC is positive).

2) Synchronization Tracking: After the initial synchronization, the hardware removes the first N_c samples of each symbol. Note that the transmitter added a cyclic suffix, but the receiver removes a cyclic prefix. This results in a cyclic shift of the data part of the symbol in the time domain or a phase rotation in the frequency domain.

The channel is estimated once per frame using the SCH symbol at the beginning of the frame. The channel is estimated in the frequency domain by multiplication of the received symbols with the complex conjugate of the pilots. A time-domain channel estimate is obtained by applying an FFT.

Due to the drifts of the sampling clocks of transmitter and receiver, as well as the movement of the user, the synchronization needs to be adjusted constantly. This is done by tracking the peak of the channel estimate in the time domain. To avoid jitter, the peak position is passed through a low-pass filter. If the peak position drifts from the target position by more than 5 samples, the timing offset of the hardware is increased (decreased) by one sample. Due to the

cyclic shift of the symbol, under perfect synchronization, the peak of the time domain channel estimate would be at sample $N_d - N_c$. The target peak position is thus set to $N_d - 7/8N_c$.

After synchronization tracking, the receiver demodulates and decodes the BCH. If the BCH cannot be detected successfully for 100 consecutive frames or more, the receiver declares itself out of sync and the initial synchronization procedure is stared again. For successful decoding of the BCH, a SNR of approximately 10 dB or more is required.

3) Multi-user Synchronization: In order to conduct multi-user measurements, all the UEs need to be frame-synchronized to the BS. This is important for (i) synchronized start and stop of the data acquisition and (ii) for the proper alignment of the measurement data from multiple users in the post processing. Multi-user synchronization is achieved by using the frame number encoded in the BCH. This frame number is also stored along with the measured channel at the UEs for post processing.

D. Automatic Gain Control

The automatic gain control adjusts the gains of the AD converters in steps of 5 dB such that the received digital power is approximately 43 dB. This way saturation of the AD converters is avoided. The calibrated total gain of the receive chain is stored along with the measurements.

E. Channel Estimation Procedure

Once the receiver is synced with the transmitter, the EMOS channel estimation procedure is started. Therefore we use not only one SCH symbol, but all 48 pilot symbols in the transmit frame. This increases the quality of the channel estimation.

The channel estimation procedure consists of two steps. First, the phase-shift noise generated by the dual-RF CardBus/PCMCIA card is suppressed using a phase derotation. Generated by the RF circuit, the phase-shift noise was observed to have a slow variation characteristic. We therefore model the phase-shift noise as being constant for each OFDM symbol and different for different OFDM symbols. We calculate the phase shift of every pilot symbol with respect to the first pilot symbol, which is used as a reference.

Secondly, channel is estimated for each receive antenna based on the average of the 48 pilot symbols. Since the SNR at the receiver is at least 10 dB, the total measurement SNR is at least $10 + 10 \log 48 \approx 27$ dB. The estimated MIMO channel is finally stored to disk. For a more detailed description of the channel estimation see [4].

III. POST PROCESSING AND PARAMETER EXTRACTION

A. Normalization

One measurement results in the set of MIMO matrices

$$\{\mathbf{H}_{k,m,q} \in \mathbb{C}^{N \times M}, k = 0, \ldots, K-1, m = 0, \ldots, N_{\text{Frames}} - 1, q = 0, \ldots, Q-1\},$$

where k denotes the user index, m the snapshot index, and q the frequency (or subcarrier) index. $N, M,$ and K are the number of transmit antennas, number of receive antennas and number of users respectively. The total number of snapshots per measurement is $N_{\text{Frames}} = 18.700$, which corresponds to approximately 50 seconds. The total number of subcarriers is given by $Q = N_u/M$. The MIMO matrices are normalized by

$$\mathbf{H}'_{k,m,q} = \mathbf{H}_{k,m,q}\sqrt{\frac{MNN_{\text{Frames}}Q}{\sum_{m,q}\|\mathbf{H}_{k,m,q}\|_F^2}} \tag{1}$$

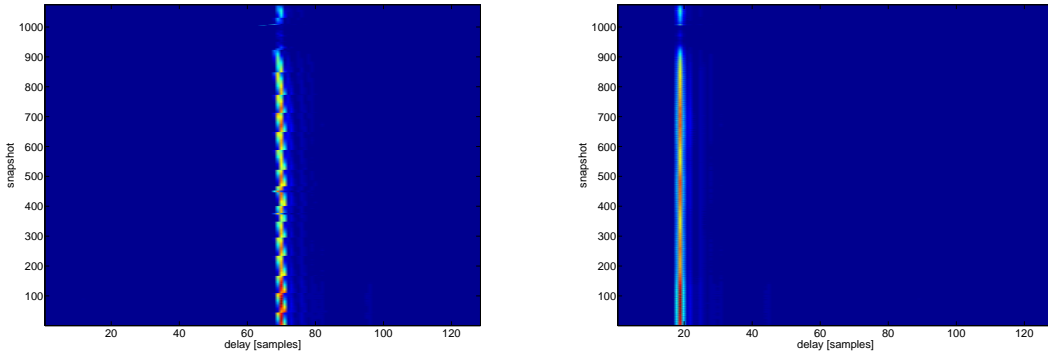such that $\mathbb{E}\{\|\mathbf{H}'_k\|_F^2\} = MN$.

Fig. 3. PDP over time for the 1st link of the 1st user: before and after re-alignment.

B. Synchronization

As described in the previous section, the receiver establishes synchronization with the transmitter using the estimation and tracking of a synchronization symbol. The timing accuracy of this procedure is in the order of a few samples. While this is enough for data detection and also capacity analysis, it is not good enough for estimation of parameters like power delay profiles.

One possible way to increase the accuracy is to re-align the impulse responses in a post processing step. Let $\mathbf{h}_{k,m,\tau}$ denote the MIMO matrix in the time-delay domain, i.e., the IDFT of $\mathbf{H}_{k,m,q}$. We oversample $\mathbf{h}_{k,m,\tau}$ in τ by a factor of 8 and align the impulse responses along their highest peak. Afterwards the impulse responses are downsampled again. This procedure is depicted in Fig. 3

This procedure will work fine in LOS scenarios, because the strongest peak will be the LOS path, which has a deterministic component. In some scenarios the strongest path might not be the LOS path and thus will be prone to fading. Synchronization can thus not be guaranteed.

C. PDP Estimation

Assuming that the channel is wide sense stationary in frequency q, the power delay profile (PDP) can be written as

$$P_{i,j,k}[m,\tau] = \mathbb{E}\{|h_{i,j,k,m,\tau}|^2\}, \tag{2}$$

where $h_{i,j,k,m,\tau}$ is the (i,j)-th element of the time-delay domain MIMO matrix $\mathbf{h}_{k,m,\tau}$.

To estimate the expectation in (2), we average over 200 consecutive snapshots (this corresponds to a movement of the user of apx. 40λ at the maximum speed of 50km/h). We thus introduce a new time variable $n = \lfloor m/200 \rfloor$ and write

$$P_{i,j,k}[n,\tau] = \frac{1}{200} \sum_{m=200n}^{200(n+1)-1} |h_{i,j,k,m,\tau}|^2. \tag{3}$$

D. Rice Factor Estimation

The Ricean K-Factor is the ratio of the strength of the deterministic component of the channel over the strength of the random part of the channel. In this work, we estimate the Ricean K-Factor using the method of moments [9].

The Rice factor can either be estimated separately for every link and every delay bin of the re-aligned impulse responses $|h_{i,j,k,m,\tau}|^2$, for every link and the total power of the impulse response,

$$g_{i,j,k,m} = \sum_{\tau} |h_{i,j,k,m,\tau}|^2, \tag{4}$$

or for the whole MIMO matrix

$$G_{k,m} = \sum_{i,j,\tau} |h_{i,j,k,m,\tau}|^2. \tag{5}$$

In this work we have decided to use the latter method. Care has to be taken to compensate for the automatic gain control, which results in

$$G_{k,m} = \sum_{i,j,\tau} |h_{i,j,k,m,\tau}|^2 \cdot 10^{-\text{rx\_total\_gain\_dB}_{k,m}/10}. \tag{6}$$

where $\text{rx\_total\_gain\_dB}_{k,m}$ is the total gain from the automatic gain control.

The number of samples used for the Rice factor estimation is a very crucial point. We have experimented with several number of snapshots from 200 as for the PDP estimation up to the total number of snapshots in the measurement. In the end we have decided to use all the snapshots in the measurement. See the results section for more details.

E. Spectral Divergence

The spectral divergence (SD) measures the distance between strictly positive, non-normalized spectral densities. It has been proposed in [5] and was used in [6] and [7] to characterize multi-dispersive channels. The parameters of our MU-MIMO system let us define different links within the set $S = \{(i, j, k) \, \forall i, j, k \in \{0, 1\}\}$, where i is the receive antenna index, j the transmitt antenna index and k the user index. For each link we obtain a different power delay profile. In order to compare them we use the SD measure. The time dependent SD between two different links l_1 and l_2 ($l_1, l_2 \in S$) is:

$$\gamma_n [l_1, l_2] = log \left(\frac{1}{T^2} \sum_{\tau} \frac{P_{l_1}[n, \tau]}{P_{l_2}[n, \tau]} \sum_{\tau} \frac{P_{l_2}[n, \tau]}{P_{l_1}[n, \tau]} \right) \tag{7}$$

where $P_l[n, \tau]$ is the power delay profile per link with n, the chunk number and τ, the delay. And T is the number of samples in the delay domain.

We define through the SD three different criterion of comparison. Given a certain user $\boldsymbol{k}$, we define the spectral divergence γ_{usr} for the links created between transmit and receive antennas, $l = (i, j, \boldsymbol{k})$. The spectral divergence γ_{rx} compares links between transmit antenna and user, $l = (\boldsymbol{i}, j, k)$, given a receive antenna $\boldsymbol{i}$. And finally γ_{link} denotes the spectral divergence between users given a certain link between transmit and receive antennas $l = (\boldsymbol{i}, \boldsymbol{j}, k)$.

IV. MEASUREMENTS AND RESULTS

A. Measurement Description

The Eurecom MIMO OpenAir Sounder (EMOS) has been used to conduct measurements in the vicinity of Eurecom, Sophia-Antipolis, France. In all measurements there were 2 (cross-polarized) Tx antennas and 2 UEs with two antennas each. A summary of the measurement parameters are given in Table II. For the analysis in this document we have selected a LOS measurement. In this measurement the UEs were walking in front of the post office in Garbejaire (see Fig. 4). The users were holding the laptops in their hands.

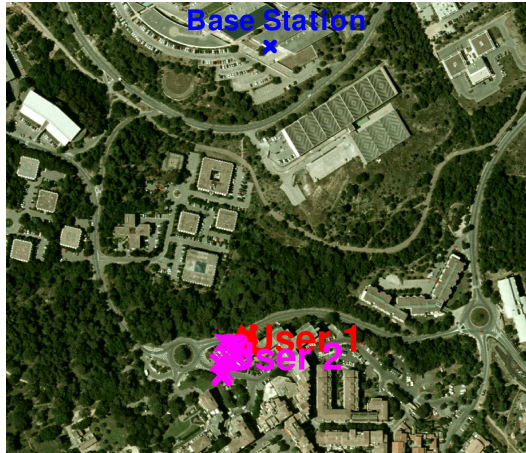| Parameter	Value
BS Transmit Power	33 dBm
Number of Antennas at BS	2 (cross polarized)
Number of UE	2
Number of Antennas at UE	2

TABLE II
EMOS PARAMETERS

Fig. 4.   Map of the measurement.

B. Results

Firstly, we plot the received signal strength of both users over time in Fig. 5. It can be seen that both users have a very high received power and it does not very significantly over the first 15.000 snapshots. After that the received power at user 2 drops approximately 20dB, which might be due to the fact that th user went out of the LOS.

1) Power Delay Profile: Fig. 6 shows the PDPs of all links of all users for chunk 50. The non-ideal system response of the EMOS is clearly visible. Also notice the measurement SNR
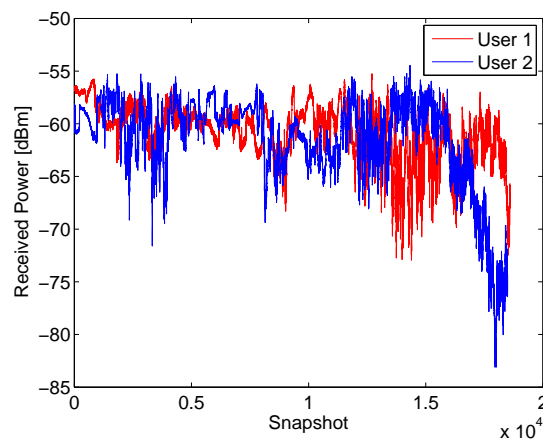

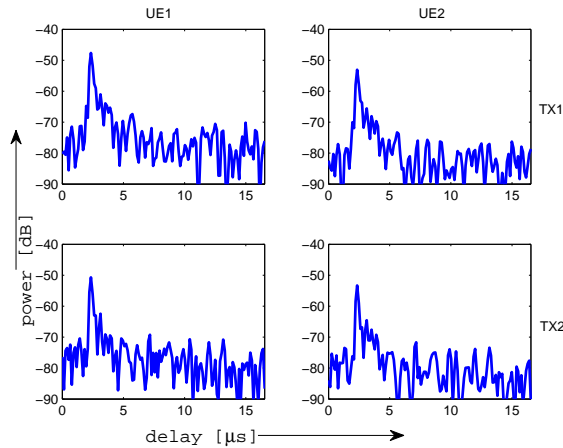Fig. 5.   Received signal strength for both users.

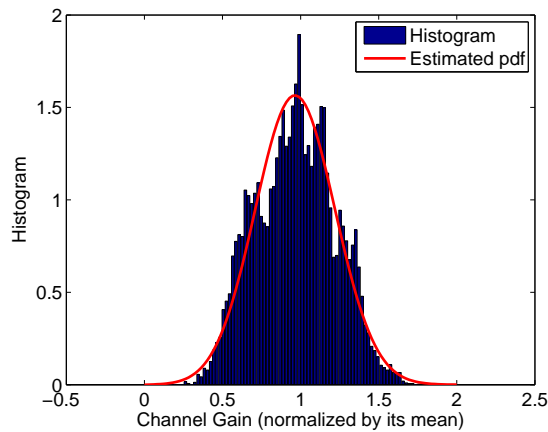Fig. 6.   PDPs of all links of all users for chunk 50.

Fig. 7.   Histogram and fitted Ricean pdf of the received signal strength (normalized to 1) of the first 15.000 snapshots of the second user.

of about 30dB.

2) Rician K-Factor: In Fig. 7 a histogram and a fitted Ricean probability density function of the first 15.000 snapshots of the second user is shown. It can be seen that the Ricean pdf fits the data rather well. The estimated Rice factor for user 1 is $K = 6.28$ and for user 2 $K = 6.4$ if only the first 15.000 snapshots are taken into account.

3) Spectral Divergence: We applied the three spectral divergences defined in Section III-E to our measurements. In Fig. 8 and Fig. 9, γ_{usr} and γ_{rx} are plotted respectively for the fiftieth chunk. When we analyze one single user (Fig. 8), we observe that the divergence is higher when considering different receive antennas. This tendency is kept over time and for different users. The chosen receive antenna determines the similarity among links. When we consider a single receive antenna but introduce another user (Fig. 9), the divergence between users increases, even though we consider the same receive antenna for both users. In this case, the tendency is also kept over time and for different receive antennas.

The last defined spectral divergence measure compares one link between users and in this case we present its time evolution. Since we are measuring the (dis-)similarity between users, it
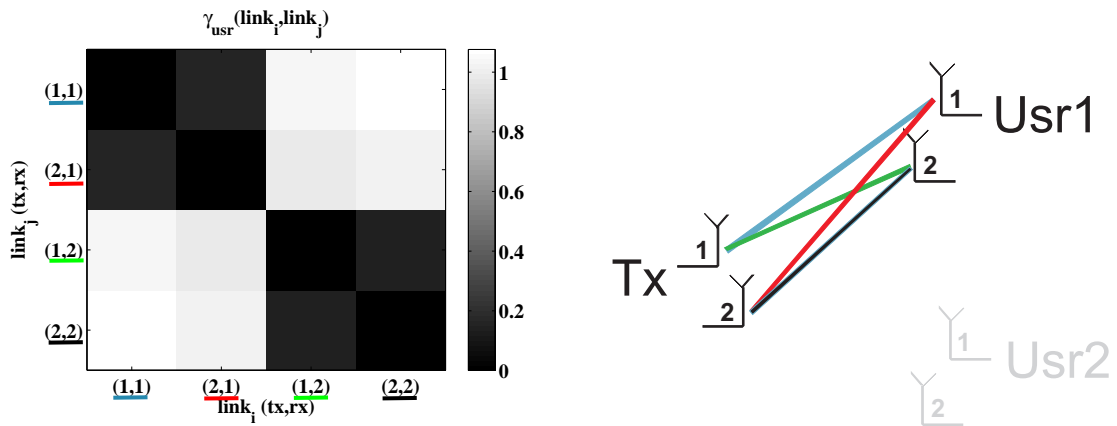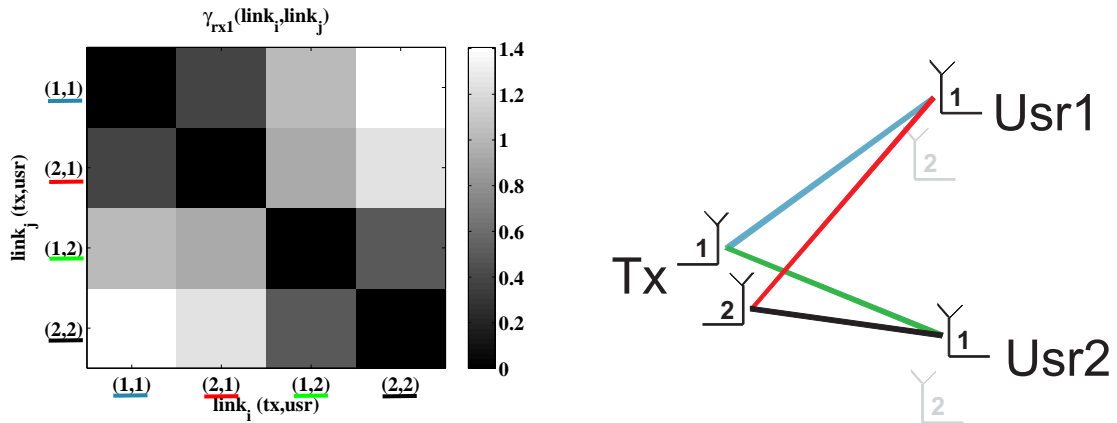
Fig. 8.   SD for user 1 of all links for chunk 50.

Fig. 9.   SD of all links of all users for chunk 50 considering the receive antenna 1.

makes sense to compare γ_{link} with the distance between them. In Fig. 10 we plot γ_{link} for the 4 possible link combinations between transmit and receive antennas (green line) and the distance between user 1 and 2 obtained from GPS data (black line). The time evolution for all links matches with the distance between users over time only for small periods of time. During them, the further the two users are, the higher the divergence is.

V. CONCLUSIONS

We have presented an analysis of measured MU-MIMO channels using the spectral divergence measure to characterize the (dis-)similarity of the channels of different users. The data was acquired using Eurecom's MU-MIMO channel sounder EMOS. The spectral divergence between PDPs from the same Rx antenna but different Tx antennas can be very low, even if the Rx antennas are at different users. However, the current measurements do not allow clear conclusions on the relationship of the distance and the spectral divergence. This might also be due to other effects such as shadowing through bodies as well as imperfect GPS data.
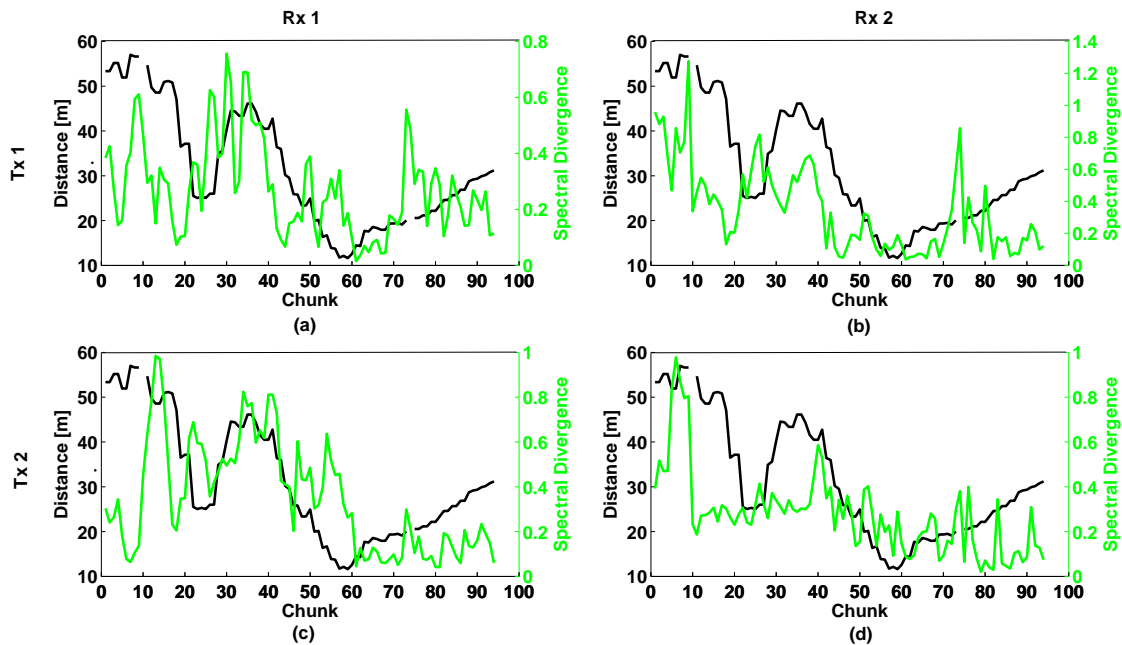
Fig. 10. Distance between users 1 and 2 (black line). Spectral divergence between users for Tx-Rx antenna links: (a) 1-1, (b) 1-2, (c) 2-1, (d) 2-2 (green line).

REFERENCES

[1] F. Kaltenberger, L. S. Cardoso, M. Kountouris, R. Knopp, and D. Gesbert, "Capacity of linear multi-user MIMO precoding schemes with measured channel data," in *Proc. IEEE Intl. Workshop on Signal Processing Advances in Wireless Communications (SPAWC)*, Recife, Brazil, Jul. 2008.

[2] F. Kaltenberger, M. Kountouris, D. Gesbert, and R. Knopp, "Correlation and capacity of measured multi-user MIMO channels," in *Proc. IEEE Intl. Symposium on Personal, Indoor and Mobile Radio Communications (PIMRC)*, Cannes, France, Sep. 2008.

[3] ——, "Performance of multi-user MIMO precoding with limited feedback over measured channels," in *Proc. IEEE Global Communications Conference (IEEE GLOBECOM 2008)*, New Orleans, USA, Nov.–Dec. 2008.

[4] R. de Lacerda, L. S. Cardoso, R. Knopp, M. Debbah, and D. Gesbert, "EMOS platform: real-time capacity estimation of MIMO channels in the UMTS-TDD band," in *Proc. International Symposium on Wireless Communication Systems (IWCS)*, Trondheim, Norway, Oct. 2007.

[5] T. T. Georgiou, "Distances between power spectral densities," Tech. Rep. arXiv:math/0607026v2, Jul 2006.

[6] G. Matz, "Characterization and analysis of doubly dispersive MIMO channels," in *Asilomar Conference on Signals, Systems and Computers*, Pacific Grove, CA, USA, Oct./Nov. 2006, pp. 946–950.

[7] L. Bernadó, T. Zemen, A. Paier, G. Matz, J. Karedal, N. Czink, C. Dumard, F. Tufvesson, M. Hagenauer, A. F. Molisch, and C. F. Mecklenbräuker, "Non-WSSUS vehicular channel characterization at 5.2 GHz - coherence parameters and channel correlation function," in *Proc. XXIX General Assembly of the International Union of Radio Science (URSI)*, Chicago, Illinois, USA, Aug. 2008.

[8] J. Koivunen, P. Almers, V.-M. Kolmonen, J. Salmi, A. Richter, F. Tufvesson, P. Suvikunnas, A. F. Molisch, and P. Vainikainen, "Dynamic multi-link indoor MIMO measurements at 5.3 GHz," in *Proc. 2nd European Conference on Antennas and Propagation (EuCAP 2007)*, Edinburgh, UK, Nov. 2007.

[9] L. Greenstein, L. Greenstein, D. Michelson, and V. Erceg, "Moment-method estimation of the Ricean K-factor," *IEEE Commun. Lett.*, vol. 3, no. 6, pp. 175–176, 1999.